Sung-Gwang Chen*

A. Galip Ulsoy
Professor.
Fellow ASME

Yoram Koren
Professor.
Fellow ASME

Department of Mechanical Engineering
and Applied Mechanics,
University of Michigan, Ann Arbor,
Michigan, 48109-2125

Error Source Diagnostics Using a Turning Process Simulator

To improve productivity and quality in machining, it is necessary to understand the interactions among machine tool components and the cutting process. This paper presents a model that characterizes interactions among the subsystems of a computer numerically controlled (CNC) lathe. The model is combined with a cutting force model to obtain a comprehensive turning simulator that simulates the cutting forces and part dimensions. A series of calibration experiments are proposed and implemented for process simulation. The simulation results are good when compared with experimental measurements. The interactions among the subunits of a CNC lathe and the cutting process are found to be potentially important.

1 Introduction

To improve productivity and quality in machining operations, strategies have been developed and utilized in various stages of design and manufacturing (i.e., machine tool design, product design, process planning, and process control [1–8]). Typically, these strategies focus only on key subsystems (e.g., structural dynamics and spindle servo drives for chatter [11], feed-servo drives for contouring control [16]) of the complete machining system. The objective of this paper is to formulate a comprehensive modeling framework that simulates interactions among components (e.g., feed drive, spindle ect.) of a CNC lathe in order to identify the machining error sources.

The machine tool system is composed of several components: the drive servo (including spindle and feed drives), the machine tool structure, the workpiece, and the cutting process. The authors believe that the knowledge of interactions among the machine tool components and the cutting process is necessary to achieve further improvements in machining productivity and quality. The role of such interactions becomes even more significant with recent trends such as high speed machining and hard turning [9–10]. During high speed machining, fast feed drives, rigid machine structures, high speed spindles, and high power spindle drives, are required to maintain machining productivity. The need for fast feed drives necessitates the use of direct drive systems for the machine table and the cutting tool and, therefore, results in larger load torques that may significantly affect the system accuracy. During hard turning, adequate machine rigidity, coupled with a rigid tool-workpiece setup, is necessary to maintain machining quality. The large cutting forces may induce tool-workpiece deflections that contribute to significant dimensional errors of the machined part.

The paper first discusses the machining error sources within the turning process. Then a comprehensive model is developed to simulate the machine/workpiece dynamics for a CNC lathe. Next, results are presented from experiments designed to calibrate the proposed model. The model is then combined with a cutting force model developed by the authors [12] to simulate errors in the machined part dimensions.

2 Error Sources in Turning

Table 1 shows the typical magnitudes and time scales associated with major error sources from the machine tool, the control, and the cutting process.

Machine Tool. The geometric and thermal errors of the machine tool, and the forced machine vibration, dominate machining accuracy in fine cutting (i.e., finish cutting with high accuracy). During fine cutting the tool motion is very slow with small cutting forces, and the structural dynamics do not affect the machining accuracy (unless the workpiece structure is very weak). Consequently, in fine cutting, the dominant factors with respect to machining accuracy are the machine tool errors (i.e., the geometric errors and thermal errors).

Such machine tool errors are not predictable at the machine design stage because they arise mainly from misalignment during machine assembly and thermal expansion during operation. Since there is still no effective method to accurately predict such machine tool errors without performing experiments, the application of the proposed machining simulator in fine cutting is realistic only in cases where the machine tool errors have been compensated and, therefore, do not affect the part accuracy. This geometric and thermal error compensation issue is not addressed here, but has received extensive attention from other researchers (e.g., [6, 13]). However, such machine tool errors can be decoupled from the other error sources. For example, at the beginning of machining a new part, a cleaning cut is usually used to eliminate the form error of the mounted workpiece [14]. Forced machine vibrations are also not predictable in the early stage of machine/part design. They are produced by periodic forces either from unbalanced machine components or from the noisy cutting environment [14]. Nevertheless, such effects can be reduced through balanced dynamic components and vibration isolation.

Control. The source of machining inaccuracy caused by the controller/drive dynamics is the cutting force disturbances and the inertia of the drive and the machine table. The effect of these sources can be reduced by an interpolator with a deceleration function [15] or by an advanced feed drive controllers [16]. Programming and interpolation error sources are determined by the resolution of the CNC machine tool and, therefore, are small [15] when compared with other sources. The friction and backlash in the machine guideways and between the lead-screw and the machine table may also be serious problems for many inexpensive machine tools.

Cutting Process. Due to the demand for high productivity, one often selects high feedrates and large depths of cut, which induce large cutting forces. Therefore, the machine structural statics and dynamics dominate machining quality. Forced deflections of the machine tool/tool-holder and the workpiece/spindle may also have significant contributions to machining accuracy during heavy cutting. Such deflections can be calculated once the compliance of the machine tool is obtained. When

* Currently a consultant with A2 Automation Inc.

Contributed by the Manufacturing Engineering Division for publication in the JOURNAL OF MANUFACTURING SCIENCE AND ENGINEERING. Manuscript received Aug. 1994; revised Feb. 1997. Associate Technical Editor: S. G. Kapoor.

Table 1 Error sources in turning

Error Source	Magnitude (μm) maximal / typical	Time Const. typical	Refs.
Machine Tool			
Thermal Errors	250 / 100	~ 1 hour	[13]
Geometric Errors	100 / 50	~ 1 month	[13]
Forced Vibrations	200 / 100	~ 10 ms	[14]
Control			
Drive Servo Dynamics	200 / 50	~ 50 ms	[16]
Programming Errors	10 / 5	-	[15]
Programming Errors	30 / 10	-	[15]
Cutting Process			
Chatter	400 / 100	~10 ms	[17]
Tool Wear	50 / 25	~10 min	[18]
Machine tool Deflec.	50 / 20	~10 ms	[26]
Workpiece Deflec.	200 / 10	~10 ms	[22]

there is a compliant structure usually from a slender workpiece, the workpiece deflections caused by the cutting force may become much more significant. In addition, machine tool chatter is also one of the major constraints that limits the productivity of the turning process [17].

Tool wear is important under long term cutting conditions with high dimensional accuracy requirements [18]. However, the tool wear effect is neglected here so as to focus on the other major machining error sources. Other error sources, like the workpiece thermal expansion due to cutting process heating, are also neglected. However, such effects can readily be incorporated in the proposed simulator structure at some future date.

3 Machine/Workpiece Dynamics

We consider the construction of a model which enables the simulation of the major error sources during heavy cutting, which are forced deflections, and drive servo dynamics. In order to focus the discussion on these major sources, the other error sources in Table 1 are initially neglected. The form error of the workpiece is assumed to be negligible or to have been removed by a cleaning cut.

The configuration of a CNC turning system is described in Fig. 1. The NC part program that contains the information on the tool paths and the corresponding cutting parameters is fed into the interpolator to generate on-line reference inputs to the drive servos. The drive servos then move the cutting tool against a rotating workpiece to start the cutting. The cutting process induces cutting forces which eventually interact with the machine/workpiece dynamics. Under certain circumstances, such interactions may produce significant inaccuracies and even instability of the machining process.

This work focuses on modeling the machine/workpiece dynamics, which is considered to be the combination of three major subunits: (a) the drive servo system, (b) the machine tool structure, and (c) the workpiece structure. The machine tool structure (complex, but fixed) and the workpiece structure (simple, but frequently changing) are considered independently to simplify the task of model calibration.

Drive Servo System. The drive system dynamics is adequately modeled as a first order linear system [15, 16]. Since the traditional motion controller often adopts P or PID algorithms for each drive servo (one spindle drive and two feed drives) independently, each drive servo is approximated as a second order linear system:

$$Y(s) = \left(\frac{\omega^2}{s^2 + 2\zeta\omega s + \omega^2}\right)(U(s) + ksF(s)) \qquad (1)$$

Each of the drive servos has two inputs and one output. In the spindle drive, the reference spindle speed (u) and the load torque (F) are the inputs. The actual spindle speed is considered to be the output (y). As for the two feed drives, inputs are the reference position (u) and the load force (F), whereas the outputs are the actual table positions (y). The natural frequency, the damping, and the loading coefficient k are used to characterize the drive servo dynamics. Notice that there is a zero (i.e., the s) in the numerator with a loading coefficient k to indicate effects of the loading force or torque. Such a formulation is based upon experimental observation, since constant process load torques do not lead to steady state offsets in the speed (see Fig. 2).

Eventually, the whole drive servo system (one spindle drive and two feed drives) can be expressed in state space form (see Appendix):

$$\dot{\mathbf{x}}_d = \mathbf{f}_d(\mathbf{x}_d, \mathbf{F}_c, \mathbf{u}_c)$$
$$\mathbf{y}_d = \mathbf{C}_d\mathbf{x}_d \qquad (2)$$

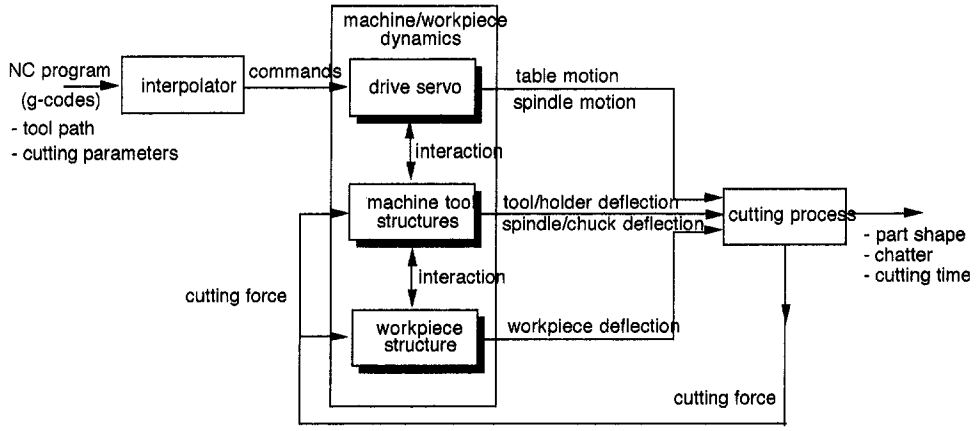

Fig. 1 The configuration of a CNC turning system

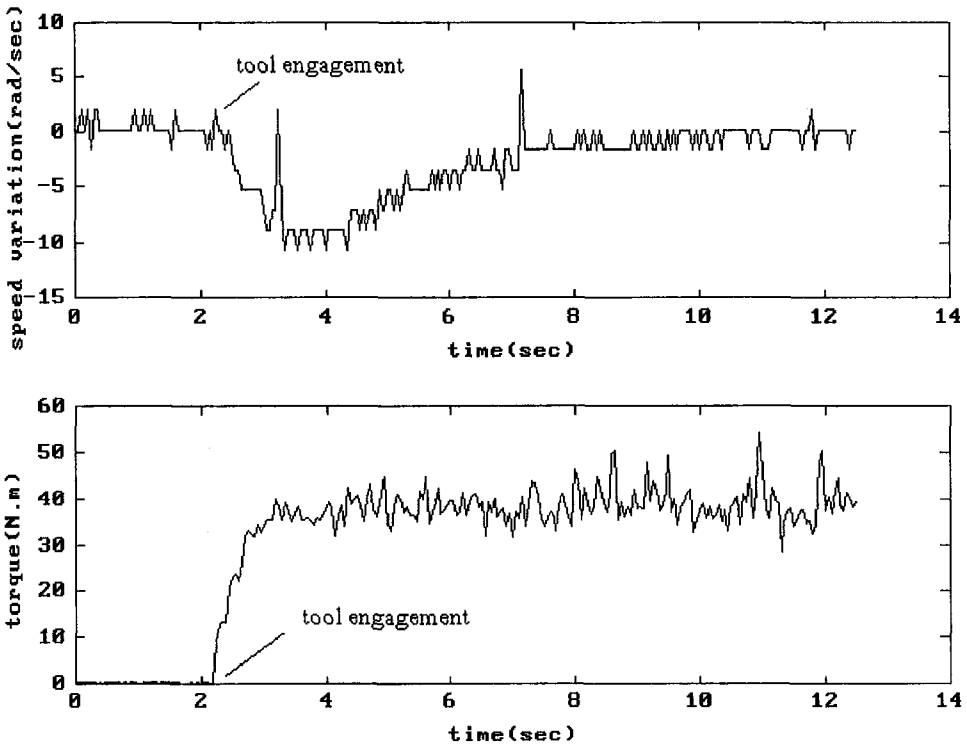

Fig. 2 Effects of the cutting load on the spindle drive servo

where t is time, $\mathbf{x}_d$ is the state vector, $\mathbf{F}_c = [F_x, F_y, F_z]'$ is the three-dimensional cutting force vector with components: radial force, cutting force, and axial feed force. The input vector $\mathbf{u}_c = [\dot{\theta}_{\text{ref}}, x_{\text{ref}}, z_{\text{ref}}]'$ consists of the reference spindle speed and machine table coordinate. The output vector $\mathbf{y}_d = [\dot{\theta}, x, z]'$ represents the actual spindle speed and table coordinate.

Machine Tool Structure. The machine tool structure is modeled as a combination of the machine tool/tool-holder structure and the spindle/chuck structure. The machine tool/tool-holder structural dynamics is quite complex [14]. Since our concern in this study is only the translational motion of the cutting edge, a linear system that describes the three dimensional motion of the cutting edge is adequate for representing the machine tool/tool-holder structural statics and dynamics:

$$\dot{\mathbf{x}}_t = \mathbf{A}_t\mathbf{x}_t + \mathbf{B}_t\mathbf{F}_c$$
$$\mathbf{y}_t = \mathbf{C}_t\mathbf{x}_t \tag{3}$$

where $\mathbf{x}_t$ and $(\mathbf{A}_t, \mathbf{B}_t, \mathbf{C}_t)$ are the state vector and the system matrices whose dimensions depend on how many vibration modes are identified in calibration experiments. The output $\mathbf{y}_t = [x_t, y_t, z_t]'$ represents the 3-D translational motion of the cutting edge.

There are several advantages to this approach:

Table 2 Calibrated model parameters of the drive servo system

Drive servo	Natural frequency	Damping	Loading coeff.(k)
Spindle	2.74 rad/sec	0.76	0.69 rad/Joule
Radial feed (x)	15.43 rad/sec	1.57	0.00 rad/N
Axial feed (z)	10.97 rad/sec	1.16	0.00 rad/N

(a) Eq. (3) can be considered the general form since it describes the cutting edge motion in three-dimensional space generally.

(b) Using identification techniques (e.g., Juang et al. [20]), one can disregard immaterial degrees of freedom easily and, hence, reduce the model size for machine tool/tool-holder dynamics. Thus, eliminating the need to solve for "stiff" system dynamics which is known to be difficult numerically.

(c) It is computationally convenient to combine Eq. (3), together with equations for other components. Since the state space formulation is suitable for numerical analysis, tedious and system-specific symbolic manipulations are avoided.

The spindle/chuck dynamics is modeled as a linear mass-spring-damper system. Since its vertical displacements are usually irrelevant to machining inaccuracy and instability [21], only the dynamics in the radial direction is considered. The notation m_S, c_S, k_S denotes the effective mass, damping, and stiffness, respectively.

Workpiece Structure. When cutting a slender workpiece, the stiffness of the workpiece structure varies slowly along the feed direction [22]. The workpiece stiffness can also vary periodically with the angular displacement of the spindle. The effect of structural parameter variations on the workpiece structure are neglected here so as to focus on studying the interactions among machining components. The workpiece is also modeled as a linear mass-spring-damper system, where m_w, c_w, k_w are the effective mass, the damping, and the stiffness, respectively. With this formulation, the stiffness can be determined using a static loading test. Effective mass and damping can be determined using a hammer test. The time-varying stiffness due to material removal is also neglected here.

Eventually, the structural dynamics of the spindle/chuck and the workpiece are integrated as two linear spring-damper systems in series. The combined structural dynamics is expressed in state space form in the time domain:

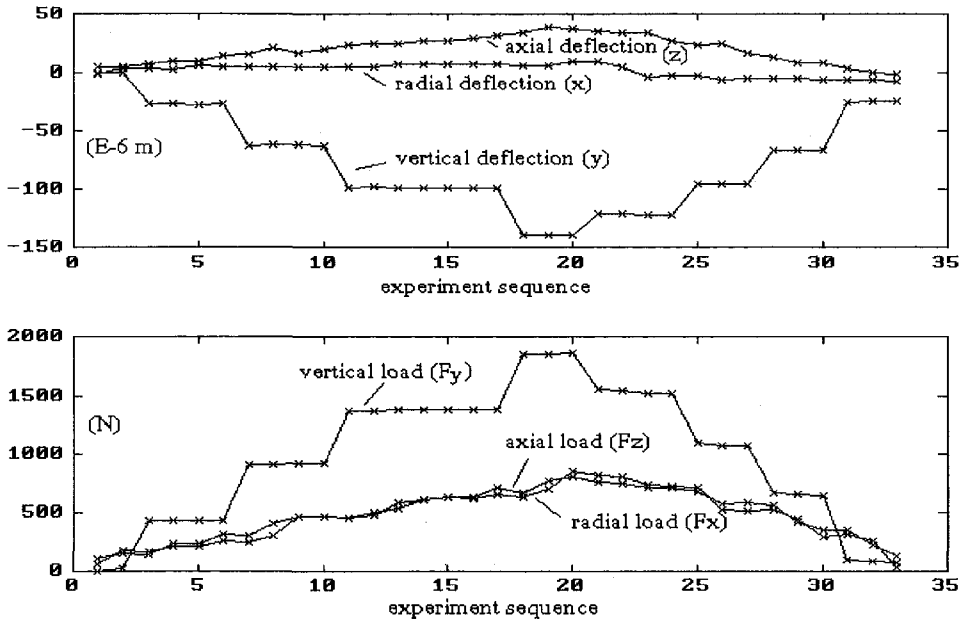

Fig. 3 Force-deflection relationship of the machine-tool/tool-holder structure in static loading

$$\dot{\mathbf{x}}_w = \mathbf{A}_w \mathbf{x}_w + \mathbf{B}_w F_x$$
$$y_w = \mathbf{C}_w \mathbf{x}_w \tag{4}$$

where $\mathbf{x}_W$ is the state vector, F_x represents the radial component of the cutting force $\mathbf{F}_c$, $y_w = x_w$ represents the radial spindle/chuck/workpiece structural deflection, and

$$\mathbf{A}_w = \begin{bmatrix} 0 & 0 & 1 & 0 \\ 0 & 0 & 0 & 1 \\ -\frac{k_s}{m_s} & \frac{k_w}{m_s} & -\frac{c_s}{m_s} & \frac{c_w}{m_s} \\ \frac{k_s}{m_s} & -\frac{m_s + m_w}{m_s m_w} k_w & \frac{c_s}{m_s} & -\frac{m_s + m_w}{m_s m_w} c_w \end{bmatrix}$$

$$B_w = \begin{Bmatrix} 0 \\ 0 \\ 0 \\ -\frac{1}{m_w} \end{Bmatrix}, \quad C_w = [1 \quad 1 \quad 0 \quad 0]$$

Further reduction of the system order can be made when one of the structures is much more compliant than the other. When the spindle/chuck is much more compliant than the workpiece, the workpiece is considered merely an additional mass m_w added to the spindle/chuck. On the other hand, when the workpiece is much more compliant than the spindle chuck, the spindle/chuck is considered a rigid support for the workpiece.

Mathematical Formulation. Combining Eqs. (2–4), the machine-tool/workpiece dynamics are formulated in terms of state equations:

$$\dot{\mathbf{x}} = \mathbf{f}_t(\mathbf{x}, \mathbf{F}_c, \mathbf{u}_c)$$
$$\mathbf{y} = \mathbf{g}_t(\mathbf{x}) \tag{5}$$

where the state vector x and the output vector $\mathbf{y}$ are defined as

$$\mathbf{x} = \begin{Bmatrix} \mathbf{x}_d \\ \mathbf{x}_t \\ \mathbf{x}_w \end{Bmatrix}, \quad \mathbf{y} = \begin{Bmatrix} \dot{\theta} \\ x + x_t + x_w \\ z + z_t \end{Bmatrix}$$

Therefore, given a cutting force model $\mathbf{F}_c(\mathbf{y}) = \mathbf{F}_c(\mathbf{g}_t(\mathbf{x}))$, for example as in [12], one is able to simulate the machining inaccuracy (i.e., dimensional errors of a machined part) and instability (i.e., chatter). However, developing general identifi-

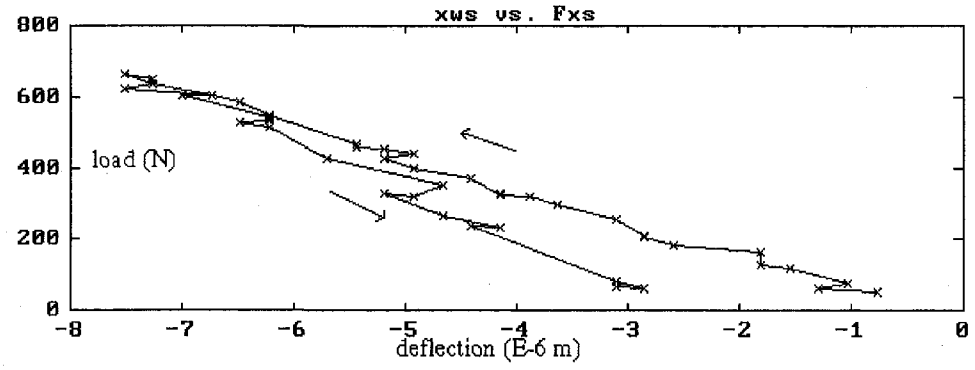

Fig. 4 Force-deflection relationship of the spindle/chuck structure in static loading

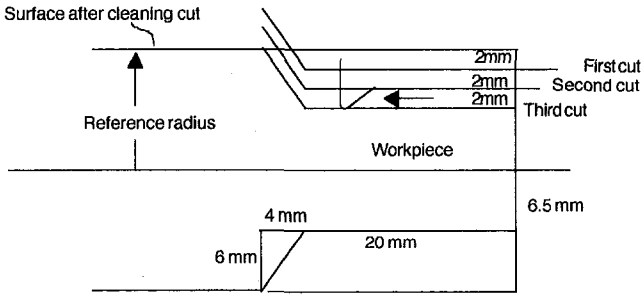

Fig. 5 Experiment design for cutting force and part dimension simulations [12]

cation techniques for machine-tool/workpiece dynamics and cutting force dynamics is still a research challenge.

In the following sections the calibration of the simulator is described, and then results are presented for experimental validation of the simulated forces and dimensional errors.

4 Model Calibration

A CNC lathe without a tail stock was calibrated in order to assess the proposed formulation. It is driven by a 30 hp DC motor which provides spindle speeds up to 3,000 rpm, and it is controlled by a CNC controller. Utilization of the turning process simulator will depend on how efficiently and how accurately the parameters of the subunits of the machining process model are identified. Therefore, it is necessary to provide an efficient way of calibrating the process parameters. Appropriate calibration experiments were performed as described below.

Drive Servo Dynamics. The damping and natural frequency of each drive servo were determined via machine idle running tests. The model parameters of the drive servo dynamics were estimated by an estimation scheme using the least square error principle [23]. The spindle drive damping and natural frequency were estimated by measuring the spindle speeds subject to a step change of the reference from zero to a certain constant value. For the two feed drive servos (x and z), the damping and natural frequency of each feed drive servo were estimated by measuring the feed strokes subject to a straight line motion command.

The spindle loading coefficient was determined by integrating the spindle variations subject to a longitudinal cut. Similarly, the loading coefficients of the radial and axial feed drives were determined via a facing cut and a longitudinal cut, respectively. The results obtained from the experiments are listed in Table 2. The spindle drive servo is an underdamped system, while the two feed drive servos are over-damped systems. The loading coefficient values show that the spindle speed is sensitive to the cutting torque, while the two feed drive servos are insensitive to cutting loads.

Fig. 2 depicts the variations of the spindle servo motions subject to the cutting load. The load torque is not shown, but is a steady value of 40–50 N.m after tool engagement. The spindle speed, due to tool-workpiece engagement, drops by 100 rpm. Such significant transient variations in speed could lead to machine tool chatter, since it is a function of the spindle speed and cutting speed [24].

Machine Tool Structure. The static compliance and dynamic parameters of the machine tool structure was determined by performing static loading and interrupted cutting tests, respectively. In both tests, "internal" loads or excitations were generated to simulate actual cutting.

In the static loading test, the loads in the radial (x) and feed (z) directions were generated by commanding the feed drive servos to move the cutting tool against the workpiece, and the cutting direction (y) load was generated by commanding the spindle drive servo to rotate the workpiece against the cutting tool. A rigid workpiece was selected to eliminate the effect of workpiece compliance. The static loads were measured by a triaxial dynamometer installed on the machine tool. The absolute displacements of the workpiece and the spindle/chuck during cutting operations were measured by non-contact capacitance sensors fixed on an independent rigid stand so that the general structural deformation of the system (two-dimensional motions in the spindle/chuck, and three-dimensional motions in the cutting tool) can be measured. The test was performed by gradually increasing and decreasing the load. The directional stiffness in the cutting (y) and axial (z) directions were estimated to be 1.8×10^7 N/m and 3.1×10^7 N/m, respectively. However, the measured radial deflections of the tool/tool-holder structure were not significant enough for compliance estimation (see Fig. 3). Therefore, another loading test was also conducted by commanding the cutting tool to push against the workpiece along the radial direction only. The tool/tool-holder stiffness was then determined to be 6.7×10^7 N/m by measuring the corresponding radial loads and displacements. The spindle/chuck compliance was calibrated by gradually varying the radial load (F_x) to obtain a stiffness of $k_s = 1.0 \times 10^8$ N/m (see Fig. 4). Note in Fig. 4 that the deflection did not return to zero after the load was removed. This is due to slight slippage of the workpiece with respect to the chuck under the static load.

The interrupted cutting test was to determine the dynamic parameters (i.e., damping, natural frequency) of both the machine-tool/tool-holder and the spindle/chuck structures. Since the machine tool at rest, in idle running, and during cutting have different structural dynamics characteristics [25], interrupted cutting operations were performed to provide "internal" excitations and an excitation energy which is closer to the real cutting energy when compared with hammer tests [25, 26]. A rigid workpiece with a notch was clamped on the chuck such that the tool cut the workpiece once per revolution with a very short cutting time to simulate impulse excitations. The vibrations of the machine-tool/tool-holder and the spindle/chuck structures, immediately after interrupted cutting, were recorded by a triaxial accelerometer and capacitance sensors. The dynamic parameters were then determined by applying the Eigensystem Realization Algorithm [19, 20].

In the machine-tool/tool-holder structure, since there is only one obvious fundamental vibration mode in the cutting direction, the corresponding damping and natural frequency are 0.04 and 794 Hz, respectively. This is consistent with the results from the static loading test that the cutting directional (y) structure has the maximal compliance. Since the radial directional (x) structure is of the main concern to machining inaccuracy and instability, the dynamics of the machine-tool/tool-holder structure are neglected in this case. Only the radial static stiffness of 6.7×10^7 N/m is considered. As for the spindle/chuck structure, the corresponding damping and natural frequency are estimated to be 0.05 and 742 Hz, respectively. The corresponding effective mass m_s and damping c_s are then calculated to be 4.6 kg and 2145 N·sec/m. Generally speaking, the machine tool structure in this case is rather rigid when compared with many machine tools [26].

Workpiece Structure. To measure the workpiece compliance, an AISI 1020 steel bar of hardness 172 HB, diameter of 25.4 mm (1 inch) and a 100 mm overhang was clamped on a rigid structure to simulate the clamping condition on the CNC lathe. The load was gradually increased by putting weights near the free end of the workpiece. The corresponding workpiece deflections were measured by a dial gage indicator. The work-

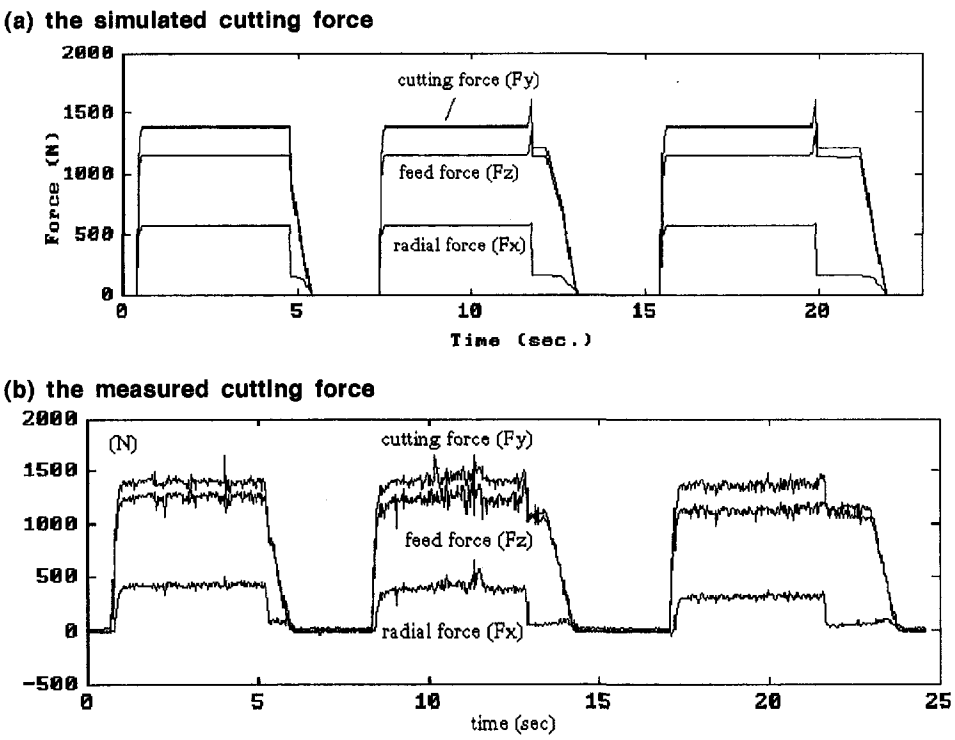

Fig. 6 The simulated and measured cutting forces [12]

piece stiffness was then determined from the known loads and from the measured deflections to be 2.9×10^6 N/m. The damping ratio and natural frequency of the workpiece structure were estimated using a hammer test and accelerometer (0.01, and 1250 Hz, respectively). The effective mass and damping are calculated as 0.047 kg and 7.38 N·sec/m.

Coupling Among Structural Subunits. The coupling among structural subunits was found to be important in the calibration experiments, and should be avoided by applying "internal" loads. For example, consider the structural interactions among the machine-tool/tool-holder, the spindle/chuck, and the workpiece in the radial direction. The "coupling" spring k_c and damper c_c should not be active for cutting operations since the real cutting force is an "internal" load, i.e., $F_1 = F_2 = F_x$, to the system. The coupling stiffness k_c was determined to be 2.9×10^7 N/m by measuring the displacement of the workpiece subject to the external load. The series-link stiffness $k_t k_c/(k_t + k_c)$, was determined to be 2.0×10^7 N/m by measuring the corresponding displacement in the tool/tool-holder structure. Given the coupling stiffness k_c and the series-link stiffness $k_t k_c/(k_t + k_c)$, the tool/tool-holder stiffness k_t was calculated to be 5.9×10^7 N/m.

5 Part Dimension Simulation

With the machine/workpiece dynamics in Eq. (5), the part dimension simulation is carried out using a tapering cut force

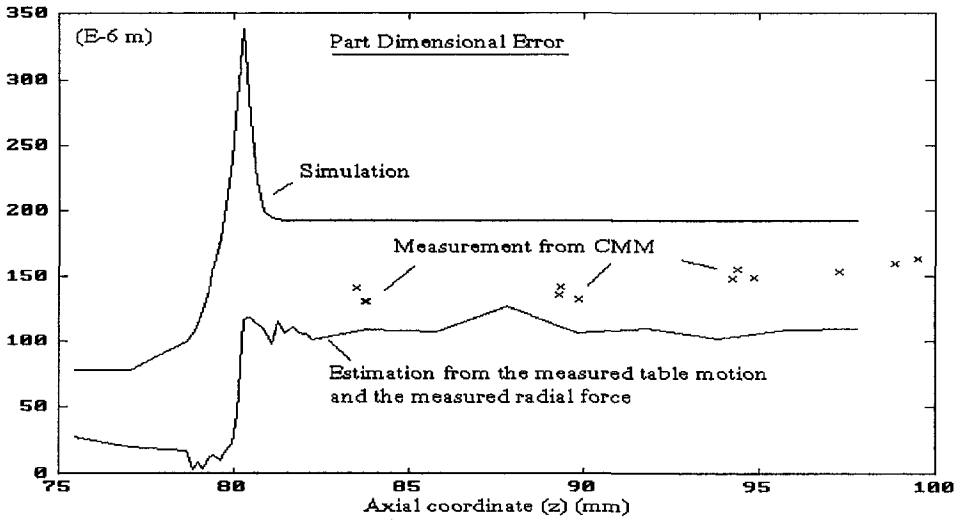

Fig. 7 The simulated and measured part dimensions

model proposed by the authors [12, 19]. The effects of workpiece geometry which come from forging or casting, of rake and lead angles and nose radius in the cutting tool, and of the tool motion kinematics, are all considered in this model. The three components of the cutting force are modeled as proportional to the instantaneous uncut chip area which can be evaluated numerically even for a complex cutting geometry.

An AISI 1020 steel bar of diameter 25.4 mm and 100 mm overhang was clamped on the CNC lathe. A Valenite 370 triangular insert was chosen such that the back rake, the side rake, the lead angle, and the nose radius are −7 deg, −7 deg, 0 deg, and 0.7938 mm, respectively. Contouring cuts were performed to shape the workpiece with a constant spindle speed of 1400 rpm, and a constant feed of 0.2 mm/rev (see Fig. 5).

The workpiece radius right after the cleaning cut was used as a reference so as to eliminate geometric errors. Note that machine thermal errors were insignificant due to the short cutting time (<30 seconds). Then three contouring cuts were performed to shape the workpiece. The three force components were measured and compared with the simulation results (see Fig. 6) using the Matlab-386 software. The machined part dimensions were also measured using a coordinate measurement machine (CMM) and compared with the simulation results (Fig. 7).

The dimensional errors were determined by the cutting contour on the workpiece, which was simulated by adding the radial structural deflections to the table positions. The dimensional errors resulting from the pure simulation, from the estimation based upon the measured table positions and radial forces (used to estimate structural deflections), and from the CMM measurements, are depicted with respect to the axial coordinate (z) in Fig. 7. Positive values indicate over sized errors. It is the third cut that contributes the most to the part dimensional errors by deflecting the workpiece. The simulated high peak error is because the simulator does not simulate the acceleration/deceleration functions in the interpolation scheme. When compared with the CMM measured results, the over simulated steady state errors are due to the workpiece deflections subject to over estimated radial forces [12]. On the other hand, the dimensional errors estimated via the measured table motions and cutting forces are less than the real measurements. This occurs because the stiffness during the last cut is smaller than the stiffness before cutting due to metal removal. When using the measured stiffness before cutting, the dimensional error will be under estimated.

6 Summary and Conclusions

A comprehensive model, and a systematic calibration methodology, has been formulated to characterize machine/workpiece dynamics. When integrated with an appropriate cutting force model, it forms the basis for a turning process simulator which simulates machining inaccuracy and instability caused by forced deflections, drive servo dynamics, and machine tool chatter. The simulation results are reasonably good when compared with experimental measurements. Therefore, the following conclusions can be drawn:

1. The proposed turning process simulator is a useful tool for machining error source diagnostics. Effects of design or process changes on machining errors can be readily assessed using the calibrated simulator.
2. The interactions among the subunits of a CNC lathe and the cutting process have been found to be potentially important for predictions of chatter, forces and part dimensional errors.

Acknowledgments

The authors are pleased to acknowledge financial support from the NSF Industry/University Cooperative Research Center for Dimensional Measurement and Control in Manufacturing.

References

1 Spur, G., Knupfer, S. U., and Schule, A., 1990, "Evaluation of Machine Tool Design Using Simulation Systems," ASME PED 45:47–53.

2 Henkin, A., and Datsko, J., 1963, "The Influence of Physical Properties on Machinability," ASME JOURNAL OF ENGINEERING FOR INDUSTRY, Vol. 87, pp. 447–454.

3 Taraman, S. R., and Taraman, K. S., 1983, "Optimum Selection of Machining and Cutting Tool Variables," SME Paper No. MR83-102.

4 Weck, M., 1983, "Machine Diagnostics in Automated Production," *J. of Manufacturing Systems,* Vol. 2, No. 2, pp. 101–106.

5 Altintas, Y., and Dong, C. L., 1990, "Design and Analysis of Modular CNC System for Machining Control and Monitoring," ASME PED Vol. 45, pp. 199–204.

6 Chen, J.-S., 1991, "Real-time Compensation for Time-Variant Volumetric Error on a Machining Center," Ph.D. Thesis, The University of Michigan, Ann Arbor.

7 Shiraishi, M., and Kume, E., 1988, "Suppression of Machine-Tool Chatter by State Feedback Control," CIRP Annals, Vol. 37, No. 1, pp. 369–372.

8 Masory, O., and Koren, Y., 1985, "Stability Analysis of a Constant Force Adaptive Control System for Turning," ASME JOURNAL OF ENGINEERING FOR INDUSTRY, pp. 321–328.

9 Agapiou, J., 1991, "Full Speed Ahead," *Cutting Tool Engineering,* pp. 69–77.

10 Schmenk, M., 1992, "Hard Turning," *Cutting Tool Engineering,* pp. 56–60.

11 Olbrich, R. J., Fu, H. J., Bray, D., and Devor, R. E., 1985, "Study of A Control System with Varying Spindle Speed in Face Milling," *Proc. of the 13th North American Manufacturing Res. Conf.,* pp. 567–574.

12 Chen, S.-G., Ulsoy, A. G., and Koren, Y., 1993, "Prediction of the Resultant Contouring Force in Metal Cutting on A Lathe," *ASME Symposium on Mechatronics,* DSC-Vol. 50/PED-Vol. 63.

13 Kiridena, V. S. B., and Ferreira, P. M., 1991, "Modeling and Estimation of Quasistatic Machine-Tool Errors," *Trans. of NAMRI/SME,* pp. 211–221.

14 Tlusty, J., 1980, "Machine Tool Mechanics," *Technology of Machine Tools-Machine Tool Task Force,* Vol. 3, UCRL-52960-3.

15 Koren, Y., 1983, *Computer Control of Manufacturing Systems,* McGraw-Hill, Inc..

16 Koren, Y., and Lo, C. C., 1992, "Advanced Controllers for Feed Drives," *CIRP Annals,* Vol. 41, No. 2, pp. 689–698.

17 Marui, E., Kato, S., Hashimoto, M., and Yamada, T., 1988, "The Mechanism of Chatter Vibration in a Spindle-Workpiece System: Part 1-Properties of Self-Excited Chatter Vibration in Spindle-Workpiece System," ASME JOURNAL OF ENGINEERING FOR INDUSTRY, Vol. 110, pp. 236–241.

18 Park, J.-J., Ulsoy, A. G., 1992, "On-line Tool Wear Estimation Using Force Measurement and A Nonlinear Observer," ASME *Journal of Dynamic Systems, Measurement and Control,* Vol. 14, pp. 666–672.

19 Chen, S-G., 1993, "Machining Error Source Diagnostics Using a Turning Process Simulator," Ph.D. Dissertation, Univ. of Michigan—Ann Arbor.

20 Juang, J., and Pappa, R. S., 1985, "An Eigensystem Realization Algorithm (ERA) for Modal Parameter Identification and Model Reduction," *Journal of Guidance, Control, and Dynamics,* Vol. 8, pp. 620–627.

21 Kuster, F., and Gygax, P. E., 1990, "Cutting Dynamics and Stability of Boring Bars," *CIRP Annals,* Vol. 39, No. 1, pp. 361–366.

22 Doi, M., Nov. 1985, "A Study on Parametric Vibration in Chuck Work," *Bulletin of JSME.* Vol. 28, No. 245, pp. 2774–2780.

23 Astrom, K., and Wittenmark, B., 1990, *Computer Controlled Systems,* Prentice-Hall.

24 Chen, S.-G., Ulsoy, A. G., and Koren, Y., 1993, "Computational Stability Analysis of Chatter in Turning," ASME JOURNAL OF ENGINEERING FOR INDUSTRY, *in press.*

25 Chiriacescu, S. T., 1990, *Stability in the Dynamics of Metal Cutting,* Elsevier Science Publishing Company, Inc., New York.

26 Minis, I. E., Magrab, E. B., Pandelidis, I. O., 1990, "Improved Methods for the Prediction of Chatter in Turning—Part 1: Determination of Structural Response Parameters," ASME JOURNAL OF ENGINEERING FOR INDUSTRY, Vol. 112, pp. 12–20.

APPENDIX

This appendix derives Eq. (2), which describes the complete drive servo dynamics. First note that the transfer function of a drive servo in Eq. (1) can be represented in state space form as,

$$\dot{\mathbf{x}} = \mathbf{A}\mathbf{x} + \mathbf{B}\begin{Bmatrix} u \\ f \end{Bmatrix}$$

$$\mathbf{y} = \mathbf{C}\mathbf{x}$$

where

$$\mathbf{A} = \begin{bmatrix} 0 & -\omega^2 \\ 1 & -2\zeta\omega \end{bmatrix}, \mathbf{B} = \begin{bmatrix} \omega^2 & 0 \\ 0 & -k\omega^2 \end{bmatrix}, \text{ and } \mathbf{C} = [0 \quad 1].$$

If the input and output vectors are defined as:

$$\mathbf{u}_d = \begin{Bmatrix} \dot{\theta}_{ref} \\ T \\ x_{ref} \\ F_x \\ z_{ref} \\ F_z \end{Bmatrix}, \quad \mathbf{y}_d = \begin{Bmatrix} \dot{\theta} \\ x \\ z \end{Bmatrix},$$

the entire drive servo system (one spindle drive and two feed drives) can be expressed as

$$\dot{\mathbf{x}}_d = \begin{bmatrix} \mathbf{A}_s & \mathbf{0} & \mathbf{0} \\ \mathbf{0} & \mathbf{A}_r & \mathbf{0} \\ \mathbf{0} & \mathbf{0} & \mathbf{A}_a \end{bmatrix} \mathbf{x}_d + \begin{bmatrix} \mathbf{B}_s & \mathbf{0} & \mathbf{0} \\ \mathbf{0} & \mathbf{B}_r & \mathbf{0} \\ \mathbf{0} & \mathbf{0} & \mathbf{B}_a \end{bmatrix} \mathbf{u}_d$$

$$\mathbf{y} = \begin{bmatrix} \mathbf{C}_s & \mathbf{0} & \mathbf{0} \\ \mathbf{0} & \mathbf{C}_r & \mathbf{0} \\ \mathbf{0} & \mathbf{0} & \mathbf{C}_a \end{bmatrix} \mathbf{x}_d$$

where $\mathbf{x}_d$ is the state vector, the subscripts s, r, a represent the spindle drive servo, the radial feed drive, and the axial feed drive, respectively. Also notice that the loading torque can be expressed as $T = x \cdot F_y$ if the structural deflections are neglected. Therefore, the system dynamics become nonlinear, and are expressed in terms of Eq. (2).